13th World Conference on Earthquake Engineering
Vancouver, B.C., Canada
August 1-6, 2004
Paper No. 1708

GUIDELINES FOR SEISMIC ASSESSMENT OF DAMAGED BUILDINGS

Paolo BAZZURRO[1], C. A. CORNELL[2], Chuck MENUN[3] and Maziar MOTAHARI[4]

SUMMARY

Structural post-earthquake functionality is conventionally evaluated by trained engineers via visual inspection of the damage. A building is tagged "Green" (unrestricted access), "Yellow" (restricted access), or "Red" (no access) according to the severity of the observed damage. Whether the damage implies an actual decay in safety level of the building occupants during aftershocks is essentially left to judgment. We propose to use engineering analyses performed *prior* to an earthquake to determine the level of degradation in building safety implied by several different damage states. We use the *loss of capacity* (in ground motion terms) associated with each damage state as the quantitative measure of degradation. The likelihood that an *aftershock* will exceed a specific (reduced) capacity provides an objective criterion for assigning the appropriate tagging condition to that damage state. This knowledge can help engineers decide on the appropriate occupancy status should a given damage state be observed during an inspection after an earthquake. This methodology has another practical application. The same engineering analyses can also identify the level of *mainshock* ground motion expected to produce any damage state. Because a damage state can be associated with a tagging condition as explained above, this procedure also identifies the mainshock ground motion level that is expected to drive the intact building into a given tagging condition. Hence, after appropriate consideration of uncertainty in building response and capacity, one can use this information to develop fragility curves for green, yellow, and red tags, and for collapse of the intact building. A convolution of such fragility curves with the building site seismic hazard provides an estimate of the frequency of future building access restrictions and collapse. Such information is valuable when estimating the likelihood of loss of functionality of a critical facility or downtime of a building for expected loss estimation purposes.

INTRODUCTION

A few references are available in the literature (e.g., ATC-20 [1], and FEMA 352 [2]) that present procedures for post-earthquake evaluation of buildings. In all the cases post-earthquake decisions regarding short-term occupancy of buildings rest solely on engineering judgment exercised by professionals that visually inspect the facility in the aftermath of the damaging event. So far little

[1] Manager Engineering Analysis, AIR Worldwide Co., 388 Market Street, Suite 610, San Francisco, CA, USA. E-mail: pbazzurro@air-worldwide.com
[2] Professor, Dept. of Civil and Environmental Engrg., Stanford University, Stanford, CA, USA
[3] Assistant Professor, Dept. of Civil and Environmental Engrg., Stanford University, Stanford, CA, USA.
[4] Former Ph.D. Student, Dept. of Civil and Environmental Engrg., Stanford University, Stanford, CA

analytical work has been done to provide tools for inspectors to help deciding whether to permit, restrict, or deny building occupancy given the level of observed damage in the building. In our opinion an informed decision can hardly be made without considering, implicitly or explicitly, the likelihood that a building brought into a specific damage state by an earthquake may collapse during aftershock ground shaking. Therefore, we believe that a procedure that couples a sound estimation of the residual capacity of a damaged building after the mainshock with aftershock ground motion hazard at the building site is essential for rationalizing the assessment of building use restrictions after earthquakes.

Within the Pacific Engineering Earthquake Research (PEER) Center – Lifelines Program, we have developed guidelines (Bazzurro *et al*. [3]) for Pacific Gas & Electric (PG&E), the largest electric power distribution company in California, that tackle the issue of "tagging" damaged buildings. The guidelines deliver a platform for assessing more rationally whether access to buildings that are common in the PG&E building inventory should be granted or denied. These guidelines are proposed to help inspectors in making an informed decision and, of course, are not intended in any way to replace their engineering intuition regarding the safety of the damaged building in relation to short-term occupancy. These guidelines, which were developed for fairly stiff, mainly one-to-three-story buildings (e.g., steel frame buildings with concrete infill walls, concrete tilt-up buildings, prefabricated metal buildings, and steel frame buildings), such as the majority of those owned by PG&E, are applicable to all structure types, residential, commercial, and industrial alike, with perhaps the exception of tall, flexible buildings.

The building tagging issue, however, is only an intermediate step necessary to achieve the far more ambitious PG&E goal of realistically evaluating the likelihood that their power distribution network may be disrupted in the first 72 hours following a large earthquake in Northern California, in general, and in the San Francisco Bay Area, in particular. Restriction of access to some critical control or substation buildings during the 72h-long emergency period after an earthquake would greatly affect such ability. Therefore, the tagging issue is deeply and naturally embedded in a more comprehensive methodology for computing the chance that a certain level of (*mainshock*) ground motion at the building site will cause a building to reach or exceed a specified performance *limit state* that can be associated with some level of access restrictions. For historical reasons the access restrictions are defined here in terms of the color of the placards (e.g., Green, Yellow or Red) that were widely used in past earthquakes to "tag" damaged and undamaged buildings.

PRE-EARTHQUAKE ENGINEERING EVALUATIONS AS A SUPPORT TOOL FOR POST-EARTHQUAKE BUILDING TAGGING

The inspection by professional engineers in a post-earthquake investigation with the purpose of assessing building safety is usually "blind". By blind we mean that the engineer usually has no direct knowledge of the particular building being inspected besides the experience previously gained by designing/evaluating/retrofitting other similar structures. The engineer, however, would be undoubtedly helped by knowing the results of specific engineering analyses performed on the *same* (or similar) building *before* the earthquake strikes. In particular, the engineer could be informed of certain damage patterns and residual roof drifts that are expected to occur for different levels of ground motion. This knowledge can help the search for damage in elements that may otherwise be left unchecked perhaps because of difficulty in accessing the structure. In addition the inspector could be provided with a mapping between different damage patterns of increasing severity and suggested building tags. This suggestion can be valuable when making an informed decision about building occupancy.

The three conceptual steps that make this approach feasible are discussed in the following subsections.

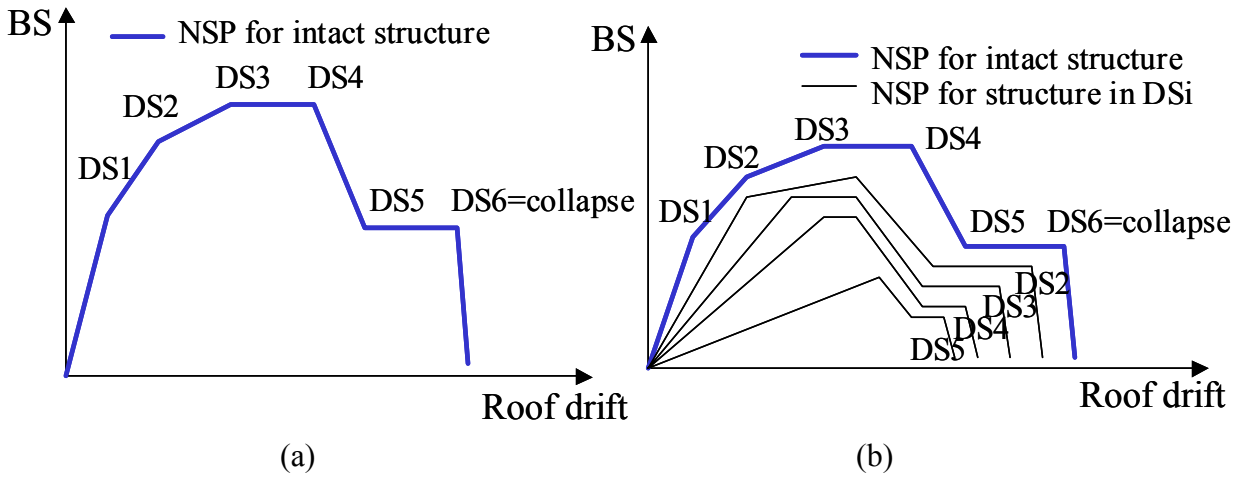

Figure 1: (a) NSP curve for the example building in its, intact, pre-earthquake condition. (b) NSP curves for the building in the pre-earthquake intact condition and in the four most relevant of all the post-earthquake damage states. For simplicity, all the curves for the damaged building have had the residual offset removed. A discussion on the effects of residual offset after the mainshock on the procedure is included in the text.

Identification of Damage States

The main assumption of this procedure relies on the principle that an exhaustive list of possible *damage states* (DS) that a building may be in after the mainshock can be identified via engineering analyses. These engineering analyses must be accurate enough to provide realistic results but not too sophisticated to be beyond the best engineering practice. In line with other guidelines (e.g., FEMA 356 [4]) we suppose that the post-elastic behavior of a building can be, to a certain extent, adequately described by the results of the Nonlinear Static Procedure (NSP) (a.k.a., pushover analysis). This assumption may be tenable for buildings that do not exceed, say, five stories in height. In particular we assume that the sequence of nonlinear events (e.g., failure of a significant portion of the roof/wall connection of a tilt-up building, fracture of at least 10% of all top flanges in a steel moment-resisting frame, or local collapse of beam-column connection due to shear failure) that develop for incremental lateral loads and the drift values at which such nonlinear events occur are reasonably well identified by the NSP curve. Some preliminary results that will be incorporated in a revision of the guidelines (Bazzurro *et al*. [3]) show that this assumption for a first-mode dominated 3-story SMRF in general holds for all damage states and more accurately so for the lower severity ones. Less agreement is to be expected for structures with significant response contribution from higher modes.

Typically the NSP curve relates the applied base shear, BS, to the resulting roof drift (i.e., roof displacement divided by the height of the building). The major inelastic events sometimes cause significant drops in the base shear or changes in the global stiffness of the building which in turn translate into changes in slope of the NSP curve, as depicted in the graph in the left panel of Figure 1. In other cases their occurrence may only moderately reduce the global stiffness of the structure and, therefore, may not produce sharp kinks in the NSP curve. For the purpose of these guidelines, the building must be "pushed" to drift levels sufficiently high to make the structure unstable (i.e., DS_6 in Figure 1) or to cause at least one element in the structure to loose its ability to carry vertical loads (e.g., shear tab failure of a beam-column connection in a steel moment-resisting frame, SMRF), whichever case come first. The global instability implies, at least numerically, the collapse of the entire building. The local loss of vertical capacity can be assimilated to a partial collapse, a less devastating failure mechanisms that can, however, still cause injuries and casualties if the building remains occupied.

These inelastic events can be grouped in a limited set of what we previously called *damage states*. More formally, the occurrence of the i^{th} major inelastic event (or a set of events at approximately the same

deformation level) identifies the i^{th} *damage state*, DS_i. DS_i is therefore defined by a roof drift value, Δ_i, and a detailed description of the structural damage associated with that event, including whether any element has reached ultimate vertical capacity.

Residual Capacity of a Damaged Building

To estimate the likelihood of building collapse (global or local) due to aftershocks, we seek to assess the building residual capacity for any damage state that could be observed after the mainshock as identified by the NSP curve. Since we intend to couple the NSP results with aftershock hazard, which is naturally expressed in terms of a ground motion parameter, it is convenient to define the residual capacity in ground motion terms as well. We use here the spectral acceleration, $S_a(T_1)$, at the fundamental initial period of vibration, T_1, of the intact building. To be precise, we intend to estimate the *median residual* dynamic lateral "capacity", $(\check{S}_{a,cap})_i$, of the damaged structure in each post-mainshock damage state DS_i to resist aftershocks. $(\check{S}_{a,cap})_i$ is the (aftershock) ground motion level that is expected to cause subsequent collapse and, should the building still be occupied, life loss. We seek an estimate of the median value but the building capacity is also affected by different sources of uncertainty as it will be discussed later.

Estimation Methodology

The estimate of $(\check{S}_{a,cap})_i$, however, cannot be directly obtained from the pushover curve, which is a representation of the nonlinear *static* behavior of a building, not *dynamic*. Conceptually, $(\check{S}_{a,cap})_i$ can be computed by performing nonlinear dynamic analyses for a set of n ground motions that are strong enough to bring the structure that is in damage state DS_i to the verge of failure and by taking the median of the n S_a values at the period T_1. The records can be either naturally at the level of severity that causes incipient collapse of the structure, or, more likely, appropriately scaled to the desired intensity level with a trial and error operation (see Luco *et al*. [5] for issues about ground motion scaling). Luco *et al*. [6] calibrated the residual capacity estimates obtained with the proposed methodology by doing just that.

We recognize, however, that nonlinear dynamic analysis is not yet widely used by practitioners. Therefore, for this purpose we use a practical tool called SPO2IDA (Vamvatsikos and Cornell [7]). This spreadsheet provides an estimate not only of the median incremental dynamic analysis (IDA) curve (Vamvatsikos and Cornell [8]) for the building but also of its record-to-record variability without the need of running any nonlinear dynamic analysis. The median IDA curve provides a relationship between ground motion level, here $S_a(T_1)$, and the building response, here gauged by roof drift. The IDA is estimated for a single-degree-of-freedom oscillator whose period of vibration and force-deformation backbone curve are the same as the building initial fundamental period of vibration and its pushover curve, respectively.

Again, we are interested in assessing the median residual capacity of a building that has already been damaged as defined, for example, by the damage state DS_i. Therefore the pushover curve input to the SPO2IDA spreadsheet must refer to the building in this post-earthquake damage state. The right panel of Figure 1 shows a cartoon of four pushover curves for the damage states DS_2 to DS_5 identified for this structure and one for the intact building. Note that the curve for DS_1 is the same as the curve for the intact building while the curve for DS_6 is meaningless given that the building is on the verge of collapse. For illustration purposes only, the pushover curves for the damaged conditions are plotted with no static offset.

Computational Aspects

Conceptually, the NSP curve for damage state DS_i can be computed in one of two ways. The first method entails loading the intact structure until the roof drift value, Δ_i, is reached, unloading it to zero base shear (which, in general, corresponds to a static offset greater than zero), and reloading it again until the building fails (Bazzurro *et al*., [3]). This method requires the use of a NSP software, such as RAM

Perform [9], that has loading and unloading capabilities. The second method (Maffei et al., [10]) does not require the use of any specialized software besides the one adopted for computing the NSP curve of the intact building. It assumes that the NSP curve for the damage state DS_i coincides with the pushover curve for the intact building for roof drifts greater or equal to Δ_i. Furthermore, the approach provides rules on how to compute the reloading stiffness and the residual drift of the NSP curve at zero base shear based on the observed damage pattern at DS_i. These rules allows one to compute manually the NSP curve for a damaged building for roof drifts below Δ_i. Theoretically, it is irrelevant for these guidelines which procedure is adopted, only the values of the residual capacity may differ.

As mentioned above, the NSP curve for a given damage state DS_i is, in general, affected by a positive residual roof drift, $(\Delta_{off})_i$, at zero base shear. The offset at the end of the mainshock means that the structure is not in a plumb position anymore. Intuitively, for the same damage pattern a large value of $(\Delta_{off})_i$ tends to make the building more vulnerable to aftershocks, as shown by Luco *et al*. [6]. Hence, its effect on $(\check{S}_{a,cap})_i$ need to be accounted for in this procedure. The SPO2IDA spreadsheet, however, does not consider oscillators that have an initial displacement offset. Therefore, the predicted value of $(\check{S}_{a,cap})_i$ has to be adjusted by an amount that is proportional to the value of $(\Delta_{off})_i$. To estimate realistic values of $(\Delta_{off})_i$ Luco *et al*. [6] have run multiple mainshock records carefully scaled to cause the same roof drift Δ_i of each damage state DS_i for a few example structures. It suffices here to say that, as expected, NSP-based $(\Delta_{off})_i$ values are upper bounds to the residual offsets predicted by dynamic analyses. That same paper provides guidance on how to calibrate NSP-based $(\Delta_{off})_i$ values vis-à-vis the dynamic ones and how to modify the SPO-based estimate of $(\check{S}_{a,cap})_i$ to account for $(\Delta_{off})_i$. It is not important for the presentation of these guidelines to include here the mechanics of such calibration. The interested reader is referred to Luco *et al*. [6] for details. The values of $(\check{S}_{a,cap})_i$ reported hereafter should be understood as already including such adjustments.

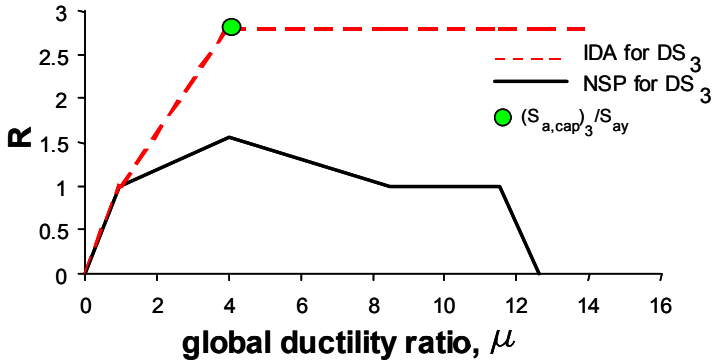

Figure 2: NSP and IDA curves for the building in the damage state DS_3 in SPO2IDA format. The abscissa represents the global ductility ratio, μ (namely, the roof drift divided by the roof drift at first yielding, i.e., at DS_1). The ordinate R is equal to BS/BS_y for the NSP curve and to $S_a(T_1)/S_{ay}(T_1)$ for the IDA curve, where BS_y and $S_{ay}(T_1)$ are the base shear and the spectral acceleration at first yielding, respectively.

Figure 2 shows both IDA and NSP curves in the same graph for the example building in damage state DS_3. Similarly to the format actually used in SPO2IDA, the drift in the abscissa and the base shear and spectral acceleration in the ordinate are normalized in the figure by their respective values at incipient yielding, namely at DS_1. For first-mode dominated structures, $S_a(T_1)$ can be found by dividing BS by the building effective modal mass for the fundamental vibration mode. Because of the methodology built-in in the SPO2IDA, this IDA estimate is accurate as long as the response of a building is first-mode dominated. This statement is reflected in the earlier word of caution regarding the questionable applicability of this procedure to tall buildings whose higher-mode contributions to the response may be significant.

As anticipated, we extract from the entire IDA curve for a damage state DS_i only the value $(\check{S}_{a,cap})_i$ at which either the curve flattens out (i.e., when the global collapse via lateral instability is reached – a similar definition was also adopted by the SAC/FEMA 350-352 Guidelines [2]) or at least one element in the building has lost its vertical capacity of carrying gravity and live loads (i.e., partial collapse). The former case is shown in Figure 2 where the value of $(\check{S}_{a,cap})_i$ (divided by $\check{S}_{ay}(T_1)$) is represented by a green dot. The same procedure repeated for all DS_i's provides an estimate of the median residual capacities at all damage states as shown in Figure 3. Besides the median curve, the SPO2IDA computes also an estimate of the coefficient of variation of $(S_{a,cap})_i$ (not shown in figure) obtained from the multitude of nonlinear SDOF analyses on which it is based.

Graphical Representation Issues

For illustrating the mechanics of this methodology it is convenient to include all the IDA curves for the intact and the damaged cases in the same plot as done in Figure 3. In order to do so it is necessary that they be expressed in terms of the same reference spectral acceleration, which in this context is chosen to be the initial elastic fundamental period, T_1, of the intact structure. For structures of moderate periods it is sufficient to assume that the ratio $S_a(T_{DSi})/S_a(T_1)$, where T_{DSi} is the fundamental period of the damaged structure in DS_i, is proportional to the inverse of the ratio of the periods, as it would be if the spectrum displayed an equal spectral velocity in this period range. Further details on this conversion are given in Bazzurro *et al*. [3]. Note that the conversion of all IDA's to the same spectral acceleration quantity is, however, computationally unnecessary. The calibration of the NSP-based $(\check{S}_{a,cap})_i$ proposed in Luco et al. [6] already implicitly takess care of this conversion.

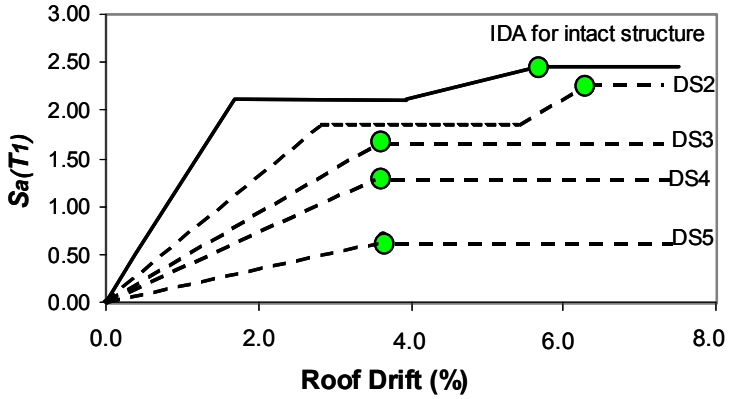

Figure 3: IDA curves for the intact structure and for the structure at different levels of damage. The circles represent for each case the estimate of the median global collapse *residual* capacity.

Definition of the Tagging Criteria

These guidelines explicitly consider five so-called structural *limit states* that are directly related to building performance. In increasing order of damage severity, they are:

- *Green tag*, G**:** the building has been inspected and deemed fit for immediate occupancy.
- *Onset of Damage*, OD: for example, FEMA 356 [4] and the HAZUS manual [11] define the onset of significant nonlinear behavior (called Immediate Occupancy in [4] and Slight Damage in [11]) for different types of structures.
- *Yellow tag,* Y**:** the building has been inspected and, until further evaluation, deemed fit for restricted occupancy. The access is limited either to specialized personnel or only to parts of the building.
- *Red tag,* R**:** the building has been inspected and deemed unsafe. No access is granted until completion of detailed engineering evaluation, retrofit or rebuilding.
- *Collapse,* C**:** the building has either collapsed (completely or in part) or is on the verge of global instability or local collapse.

The G, Y and R tag states refer explicitly to post-earthquake building functionality; the onset-of-damage state, which relates to the beginning of detectable structural damage, lies within the green-tag state boundaries; and the collapse state is, of course, the most severe stage of the red-tag condition. The OD limit state does not imply any limitations on post-earthquake building operability. It is used in the second part of the guidelines for the purpose of allowing estimates of direct financial losses in addition to indirect business-interruption losses due to downtime.

The proposed criteria for tagging damaged buildings, in whichever damage states they may be, are expressed in terms of:

- P_0, the building-site-specific mean annual frequency (MAF) of exceedance of the ground motion corresponding to the median capacity, $\check{S}_{a,cap}$, of the building in its intact conditions. P_0, which refers to the pre-earthquake conditions, can be obtained using conventional Probabilistic Seismic Hazard Analysis (PSHA) codes or directly from the *USGS website* (http://eqhazmaps.usgs.gov/) for a selected set of oscillator periods and firm-soil to soft-rock conditions.
- P, is the building-site-specific MAF of the aftershock ground motion corresponding to the median capacity, $(\check{S}_{a,cap})_i$, of the building in the damage state DS_i. P is, strictly speaking, a time-varying quantity that decreases with time elapsed from the mainshock and, therefore, it is better computed using an aftershock PSHA approach (Wiemer (2000) [12], Yeo and Cornell [13]). However, software for performing aftershock hazard is not yet widely used. For the sake of simplicity, we assume here that pre-earthquake and post-earthquake hazard do not differ. This assumption is removed in the study by Yeo and Cornell where the tagging criteria accounts for the increased probability of collapse from pre- to post-earthquake conditions due both to decreased capacity and to increased (aftershock) seismicity
- Estimates of $\check{S}_{a,cap}$ for the intact building and of $(\check{S}_{a,cap})_i$ for all the damage states DS_i's.

Tagging Criteria: Basis and Use

The proposed tagging criteria are summarized in graphical form in Figure 4.

The figure has two scales for the ordinates, the percentage of loss in $\check{S}_{a,cap}$ and the ratio of P/P_0 that measures the increase in frequency of exceeding the median residual capacity of the building damaged by the mainshock. The relationship between the two scales (see Panel b) has been tuned for coastal California sites, for which the absolute value of the (log-log) slope of an average ground motion hazard curve in the surroundings of 10^{-3} annual frequency of exceedance is about three. The hazard curve slope, which depends on the magnitude distribution and on the rate of decay of seismic waves with distance, is lower in Eastern United States, for example. Hence, in principle caution should be exercised when using this same chart in other areas of the world. The abscissa refers to the pre-earthquake conditions only; it is simply the long-term MAF of exceedance of the intact building ground motion capacity.

Before we explain the basis for the definition of the tagging "fields" in Figure 4, let us describe how the tagging criteria can be used. Any building is identified by a particular value of P_0 that can be computed during "peace" time before any earthquake has occurred. A larger value of P_0 can imply that the building is relatively "weak" or that it is located in an area of comparatively high seismicity, or a combination of both. The opposite is true for lower values of P_0. How the color of the tag changes with capacity loss can be found by searching on a vertical line at that specific value of P_0. Therefore a building whose P_0 is equal, for example, to 3×10^{-4} needs to be damaged severely enough to loose about 5% of its initial capacity before it is tagged Y and about 30% before it is tagged R. If the intact building had been much weaker or in a harsher seismic environment such that its value of P_0 were equal, for example, to 1×10^{-3}, then a nominal loss of lateral capacity of only 2% or larger would cause the building to be red-tagged. No yellow tag could be assigned in this case, either green or red.

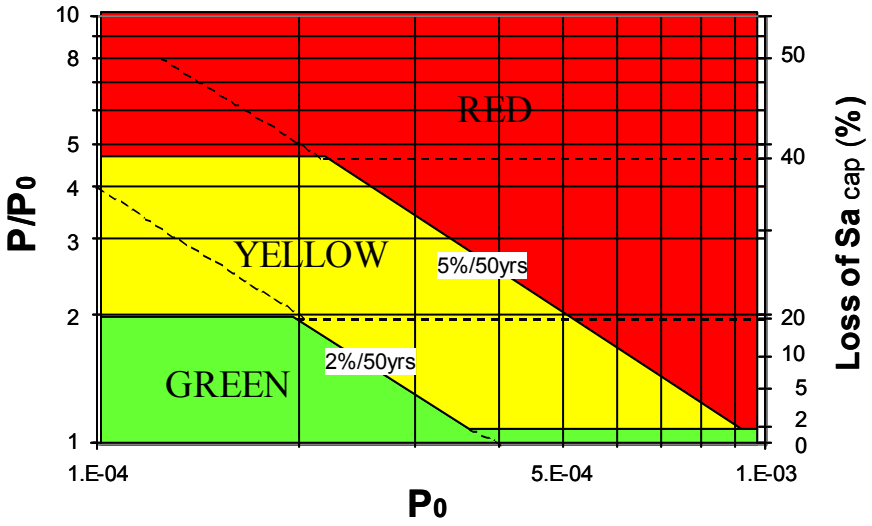

Capacity Loss (%)	P/P0
2	1.1
5	1.2
10	1.4
20	2.0
30	2.9
40	4.6
50	8.0

(a) (b)

Figure 4: (a) Graphical interpretation of the recommended tagging criteria. (b) Average relationship for loss of ground motion capacity and rate of increase in mean annual frequency of exceedance of ground motion for coastal California sites.

If the tagging criteria were simply based on maximum acceptable collapse risk of the partially damaged building, then the green, yellow, and red tag areas in Figure 4 would be oblique bands delimited by straight lines of constant *P* values. For these guidelines we selected *P* values to be equal to 2% in 50 years (mean return period, MRP, of 2,475 years) and 5% in 50 years (MRP of 975 years) for the boundaries between green and yellow tags and between yellow and red tags, respectively. These values may appear too restrictive when compared to building code requirements for new buildings that prescribe life safety as performance objective for a 10% in 50 years (i.e., MRP of 475 years) ground motion level. We selected low values to implicitly and partially account for the increased aftershock hazard that the damaged building is subject to when the inspection may take place perhaps one or two days after the earthquake. These values, which represent quantitative measures of acceptable risk, should be modified according to the building importance and severity of failure consequences.

The diagonal bands in Figure 4, however, are delimited by horizontal lines drawn somewhat arbitrarily at constant values of capacity loss of 2%, 20%, and 40%. "Weak", under-designed buildings that are potentially unsafe (i.e., larger P_0) even in pre-earthquake condition would not be tagged Y or R and possibly, at a later stage, retrofitted unless some identifiable physical damage occurred in the building. Tagging Y or R an undamaged building would be difficult to accept by owner and occupants. A hardly detectable capacity loss of only 2% encourages Y and R tagging and it is meant here to simply serve as a trigger for action for such buildings. The lines at 20% and 40%, that increase the Y and R tagging areas of "strong" (smaller P_0) buildings, have been dictated by a different concept. Results from dynamic analyses have shown, in general, that a rather widespread damage in the building is needed before the capacity drops by these amounts. In cases of widespread damage the assessment of the true building capacity is more uncertain and it is conservative to force some restriction of occupancy until further more detailed analyses are performed.

Note that a collection of figures such as Figure 4 could be produced to account for the time-varying nature of aftershock hazard. Such tagging criteria could be applicable after the earthquake at different snapshots in time when more detailed inspections and/or improved capacity analyses may take place. To mimic the decreasing aftershock hazard with time one could devise criteria that are less stringent as time

goes by. This would be reflected by a change in the constant-P lines that separate green, yellow, and red tagging areas. Criteria applicable, for example, one month after the mainshock may have constant P lines demarcating the G, Y, and R areas at higher values than those displayed in Figure 4, which is meant to be applicable immediately after the mainshock. The increased knowledge about building capacity deriving from more detailed inspection and further engineering analyses may also call for the removal of the conservative lines at 20% and 40% capacity drops in the criteria applicable at a later stage.

A final remark is in order. It is conceptually preferable to develop tagging criteria in terms of MAF of building collapse rather than MAF of *median* ground motion capacity. This entails considering the ground motion capacity as a random variable as opposed to a constant. Under certain tenable assumptions the former MAF can be computed by multiplying the latter by a "correction factor", CF, larger than one that accounts for the aleatory and epistemic uncertainties in the ground motion capacity (called β in the section to come) and the slope of the hazard curve in the neighborhood of that ground motion level. Figure 4 could still be used as is with this alternative interpretation. As a first approximation, CF can be considered to be the same for the capacities in both the intact and the damaged cases and therefore it does not have any impact on the ordinate P/P_0. For a particular application, the only change would be in the value, P_0', of the abscissa to be used to enter the graph in Figure 4, which will be larger than the MAF of exceeding the ground motion capacity, P_0, currently used. This new interpretation, which is implemented in the revised version of [3], is not carried out here in any further detail

Application: 3-story SMRF Building

As an illustrative example of this tagging methodology we used a 3-story, 3-bay SMRF (Figure 5) located in San Francisco, CA. This older building contains the kind of connections that fractured in the 1994 Northridge earthquake. Details about the building and its modeling can be found in Bazzurro *et al*. [3]. Figure 6 shows the NSP curve for the intact building with marks identifying the main damage states:

- DS_1 or Onset of Damage: it refers to the incipient yielding of the first element in the structure occurring at a roof drift of Δ_1=0.9%.
- DS_2: it is defined by the fracture of the exterior beam-column connections at the first floor that cause the first large drop in the NSP curve. This state occurs at a Δ_2=1.7%
- DS_3: it is defined by the fracture of the interior beam-column connection at the first floor. This state occurs at a Δ_3=2.4%
- DS_4: it is defined by the first failure of a beam shear tab occurring at Δ_4=4.8%. This is considered to be a partial collapse mechanism.

Figure 7 displays the NSP curves for damage states DS_2 and DS_3.. They were obtained by loading the intact structure until the roof drift specified above for each damage state was reached, by unloading it to zero base shear level, and finally by loading it again until failure (here rupture of the shear tab) occurs. Note that the software used for the NSP analyses (i.e., RAM Perform) is such that the static pushover curves for DS_2 and DS_3 return to the original intact-structure NSP curve at Δ_2 and Δ_3, respectively. This, however, may not always be the case.

The SPO2IDA-based median capacities of the intact structure and of the damaged structure in DS_2 and DS_3 are expressed in Table 1 in terms of S_a(0.73s). The values for DS_2 and DS_3 are already calibrated as suggested by Luco *et al.* [6]. Armed with this information, a site-specific hazard curve for S_a(0.73s) and, hence, the mean annual frequency of exceedance, P_0, of the capacity of the intact structure (i.e., $\check{S}_{a,cap}$=2.7g), we apply the tagging criteria of Figure 4. DS_3, with a capacity loss of 25%, is tagged Y if P_0 is below about $4\text{x}10^{-4}$ and R if above. DS_2, with a residual capacity equal to 95% of the initial capacity, is tagged G if P_0 is below approximately $3\text{x}10^{-4}$, Y if P_0 is between $3\text{x}10^{-4}$ and about $7.5\text{x}10^{-4}$, and R otherwise. If P_0 is between $3\text{x}10^{-4}$ and $4\text{x}10^{-4}$ both damage states are tagged Y, and if P_0 is greater than

$7.5x10^{-4}$ both states are tagged R. DS_2 and DS_3 are always assigned a different tag otherwise. Of course, DS_1 is always green-tagged and DS_4 is always red tagged.

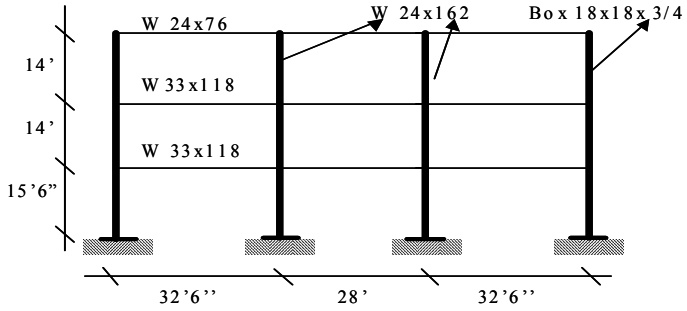

Figure 5: Schematic model of the frame

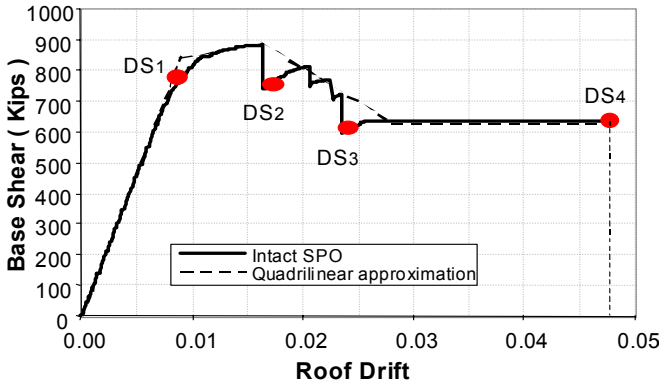

Figure 6: NSP curve for the intact structure with identified damage states DS_1 (onset of damage), DS_2, DS_3.and DS_4 (collapse).

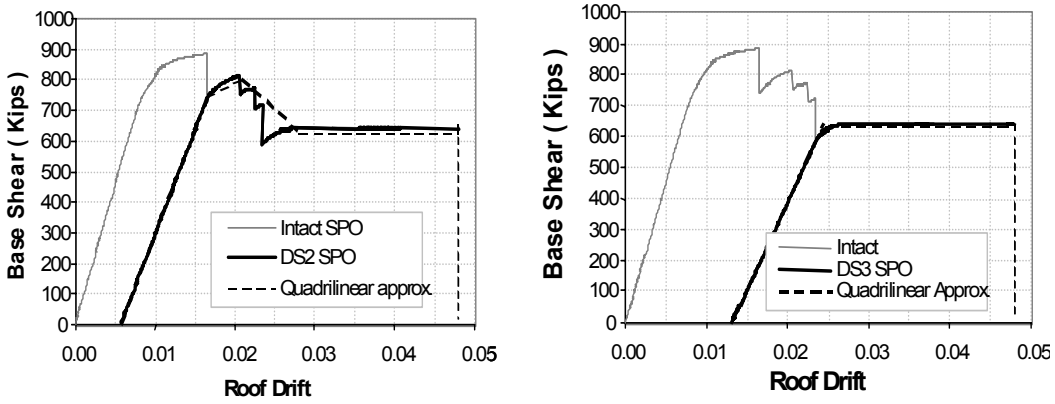

Figure 7: NSP curve for DS_2 (on the left) and for DS_3 (on the right).

Structure	$S_{a,cap}(T_1)$ (g)	Capacity Loss (%)
Intact	2.70	0
DS_2	2.55	5
DS_3	2.02	25

Table 1: Median capacities for the intact and damaged SMRF building expressed in spectral acceleration at T_1=0.73sec.

FRAGILITY CURVES FOR BUILDING TAGGING CONDITIONS

Methodology for development of fragility curves

The tagging procedure presented in the previous section uses the loss of capacity for each damage state coupled with (aftershock) hazard considerations and criteria on allowable risk to assign each *damage state* to a *limit state*. The same engineering analyses, however, can also detect the level of *mainshock* (median) ground motion expected to cause the building to reach any damage state and, therefore, any limit state (here G, OD, Y, R, and C). Hence, what has been discussed so far lends itself naturally to the development of fragility curves for limit states associated with building occupancy restrictions. A fragility curve provides the conditional probability that the intact building will be assigned a specific tag or *worse* for any given level of $S_a(T_1)$ that may be experienced at the building site. When convolved with the site hazard, the fragility curves provide the likelihood that a building can experience occupancy restrictions in a given time unit.

Figure 8 highlights the fragility curve development concepts. Panel (a) combines for our illustrative example the residual capacity in each DS_i (Figure 3) with the tagging criteria (Figure 4) specified, e.g., for a value of $P_0 \approx 2\text{x}10^{-4}$. The damage state DS_1 correspond to incipient OD, DS_2 is in G, DS_3 is in Y, DS_4 and DS_5 are in R, and DS_6 refers to incipient C. The right panel shows how this information can be used to determine the *median* spectral capacity value, $\check{S}_a^{LS}$, associated with post-earthquake tagging status for any *limit state*, LS. The value of $\check{S}_a^{LS}$ can be found immediately for OD and C whose onset correspond to one of the damage states (here, DS_1 and DS_6, respectively) by reading them off the IDA for the intact structure at the drift value of Δ_{OD} and Δ_C, respectively. The values of $\check{S}_a^{Y}$ and $\check{S}_a^{R}$, however, are not readily available because the damage states DS_i (and, therefore, Δ_i) from the NSP curve in general do not correspond to the inception of the Y and R limit states. The onset of R, for example, occurs for a damage state in between DS_3 and DS_4 (Figure 8). In this case either the procedure is repeated for one or more intermediate DS's until the computed spectral acceleration capacity is, for all practical purposes, reasonably close to the target threshold, or, alternatively but less accurately, an interpolation scheme is used instead. Finally, the value of $\check{S}_a^{G}$ is zero; any level of ground motion will generate a G tag or worse.

The ground motion spectral acceleration at T_1 at which a limit state is reached cannot, however, be predicted perfectly. The value of $\check{S}_a^{LS}$ computed above is to be considered as a "best guess" (i.e., median). It is assumed, therefore, that there is a 50-50 chance that the limit/tagging state (or worse) will be observed if this ground motion occurs at the site. There is a smaller chance at lower ground motion levels and a larger chance at higher levels. These chances are quantified by estimating the dispersion, β, which is a combined measure of two basic kinds of uncertainty: *aleatory* uncertainty (or randomness) and *epistemic* uncertainty. The former kind manifests itself, for example, in the variability in the dynamic displacements produced by different ground motion records (even though they may have the same ground motion value). Aleatory uncertainty is intrinsic in the random, unpredictable nature of earthquakes and cannot be reduced. The epistemic kind of uncertainty stems, for example, from both the limited accuracy of the selected response analysis approach and the imperfect knowledge of parameter values of the adopted mathematical model of the structure. Within the limits associated with current scientific knowledge, this second type of uncertainty can be reduced, at some expense, for example with more detailed investigation of the structure, more refined models, and more testing of material properties.

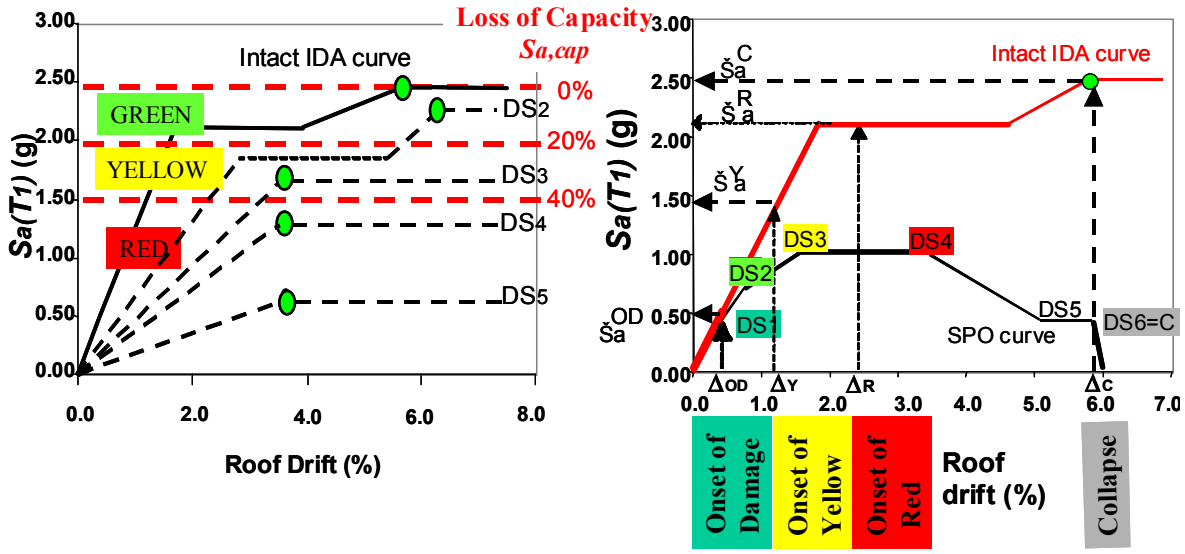

(a) (b)

Figure 8: (a) Onset of yellow and red tagging according to the criteria in Figure 4 for a structure with P_0 less or equal to about $2x10^{-4}$. (b) Median estimates of the mainshock $S_a(T_1)$ that takes the intact structure to the onset of OD, Y, R, and C. Note that, in general, the onset of a limit state may not occur exactly at the roof drift of any damage state identified by the NSP. In this case both DS3 and DS4 are beyond the onset of the yellow and red tag limit states for a structure with P_0 less or equal to about $2x10^{-4}$.

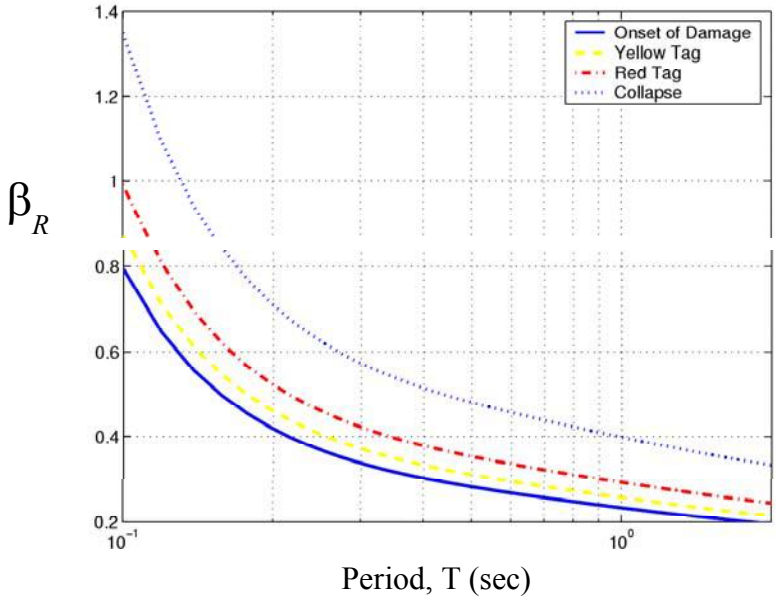

Figure 9: Recommended (default) values for β_R.

Limit State	SMRF's		Mill-type Buildings	
	Baseline	Improved	Baseline	Improved
Onset of Damage	0.3	0.25	0.7	0.4
Yellow Tag	0.6	0.5	0.8	0.6
Red Tag	0.6	0.5	0.9	0.6
Collapse	0.5	0.4	1	0.6

Table 2: Recommended (default) β_U values for SMRF and mill-type buildings.

The aleatory portion of the dispersion, β_R, depends on the initial period of vibration of the structure. Short-period structures show more record-to-record variability in their displacements (or, correspondingly, in the S_a value at which a given displacement or damage state is first observed). Further the response dispersion is larger for higher nonlinearity, especially when the ground motion is near the collapse capacity. This trend is captured by the curves presented in Figure 9. These curves are based on average results of nonlinear dynamic analyses of oscillators with different NSP backbone curves and plausible definitions of limit states corresponding to average structural deformation levels. Hence, they are suitable as β_R default values. When applying this methodology, however, the SPO2IDA spreadsheet provides structure-specific β_R values for each limit state, which can be used in place of those shown in Figure 9.

The epistemic part of the uncertainty, β_U, reflects the professional confidence that the selected model and the analysis procedure will predict accurate results. The values for β_U are larger (i.e., one will have lesser confidence) for complex, older structures characterized by a simplified model and untested material properties than for a clean, modern SMRF whose properties have been well determined and whose model has been developed with extreme care to details. Two different sets of β_U values, referred in Bazzurro *et al*. [3] as *Baseline* and *Improved*, were gathered by elicitation of expert practicing engineers and then compared with values in the literature (see references in the guidelines) for four categories of PG&E buildings: a) tilt-up or concrete block buildings (retrofitted and un-retrofitted); b) mill-type buildings (i.e., older steel frames with concrete infill walls); c) prefabricated metal buildings; and d) SMRF's. Table 2 shows the β_U values for SMRF's and mill-type buildings, values that are, respectively, the lower and upper bounds. The *Baseline* values are recommended unless the building is relatively simple (e.g., no structural irregularities), or the development of NSP curves accounts for specific characteristics of the building, such as structural irregularities or the effects of elements not typically considered part of the seismic-force-resisting system. Conditions and requirements to change the evaluation uncertainty from *Baseline* to *Improved* for each building category are also provided in [3].

The combination of the two types of uncertainties into the value of net dispersion, β, to be used in the computation of the fragility curve is done through a SRSS operation:

$$\beta = \sqrt{\beta_R^2 + \beta_U^2}$$

Given the values of β_R and β_U, the total dispersion ranges from about 0.3 when assessing the onset of damage of a very simple, moderate-period SMRF structure carefully modeled and analyzed, to more than 1.5 when estimating the collapse of older, stiff complex mill-type buildings modeled and analyzed with limited effort.

Computational aspects

Under the widely used assumption that S_a^{LS} is a lognormally distributed random variable, then the computation of a fragility curve for any LS requires two parameters: a median value $\breve{S}_a^{LS}$ and a measure of dispersion, β. The former is the central value of the curve corresponding to an exceedance probability of 50%, the latter controls its slope (the larger the β value, the flatter the curve). The evaluation of both parameters is discussed in the previous section. The fragility curve, $F_{LS}(S_a)$, for the generic structural limit state LS is determined by plotting the values of probability p = {0.05, 0.25, 0.5, 0.75 and 0.95} versus the corresponding values, S_a:

$$S_a = \breve{S}_a^{LS} e^{x\beta}$$

for the values of x equal to {–1.65, -0.67, 0.0, 0.67 and 1.65}, respectively. Additional values of p and x can be found in any table of the Gaussian distribution function.

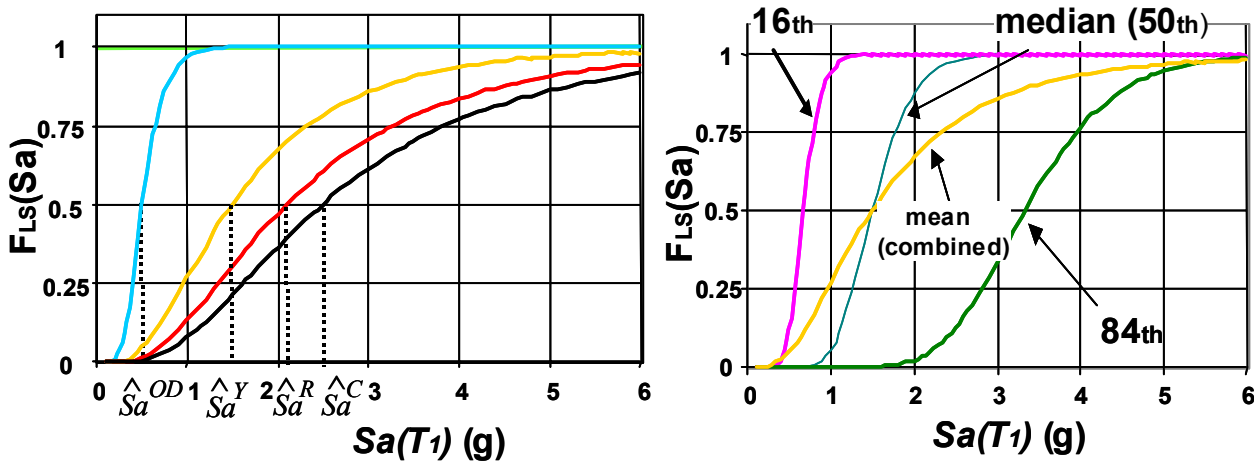

(a) (b)

Figure 10 (a) Fragility curves for onset of damage, green, yellow, and red tags, and for collapse of the building. (b) Fragility curves obtained both by separating β_R and β_U (median (50th), 16th, and 84th) and by combining them (mean).

We assume that this illustrative example consists of a SMRF building with T_1=1sec analyzed according to the specifications of the *Baseline* evaluation. We used the $\breve{S}_a^{LS}$ from Figure 8b, the β_R values from Figure 9 for T_1=0.73sec (i.e., 0.25 for OD, 0.28 for Y, 0.32 for R, and 0.43 for C), and the β_U values from Table 2 (i.e., 0.3 for OD, 0.6 for Y and R, and 0.5 for C). According to the SRSS operation defined above, the resulting β values are, therefore, 0.39 for OD, 0.66 for Y, 0.68 for R, and 0.66 for C. Figure 10a shows the resulting fragility curves for all the limit states. Note that the fragility curve for G is equal to unity for all values of ground motions. As anticipated before a building will always be at least green-tagged. The fragility curve for OD is the steepest because the value of β is the smallest. The opposite is true for the fragility curve for C.

In some applications it may be convenient to keep the epistemic uncertainty, β_U, separated from the aleatory uncertainty, β_R when computing fragility curves. If this is done, a family of fragility curves rather than one (mean) fragility curve is associated with any structural limit state. The central point of each fragility curve in this family can be computed by applying again $S_{a,y}^S = \breve{S}_a^{LS} e^{y\beta_U}$. For example, the central value, $\breve{S}_{a,y}^S$, of the median (50th), the16th, and the 84th percentile fragility curves can be found by replacing y with the values of 0, -1, and +1 in the equation above. Each fragility curve in the family can be computed using $S_a = S_{a,y}^S e^{y\beta_R}$ where now, unlike before, β is replaced by β_R. Figure 10b shows the mean fragility curve (β_U and β_R combined) along with the corresponding 16th, 50th, and 84th percentile fragility curves (β_U and β_R separated) obtained for the Y condition in the illustrative example. Of course the mean fragility curves for Y in the left and right panels coincide.

CONCLUSIONS

This article presented guidelines for rationally tagging buildings in the aftermath of an earthquake and for producing fragility curves that are related to post-earthquake building occupancy restrictions (i.e, yellow and red tags). The guidelines are generally valid for all buildings, perhaps with the exception of long-period ones, and applicable to individual buildings because they use engineering analyses performed on building-specific models. An overview of the theoretical framework necessary to extend the applicability to a generic structure of a specific building class is available in Bazzurro *et al*. [3]. The proposed tagging methodology couples the knowledge of loss in capacity of a damaged building estimated via engineering

analyses *prior* to the mainshock to considerations of aftershock hazard and acceptable risk levels for building occupancy. The time-varying nature of aftershock hazard is only implicitly considered in this article but an explicit treatment is included in the article by Yeo and Cornell [13]. The mapping between capacity loss, associated to observable damage patterns and residual roof drift, and suggested tagging is valuable to engineers that may be inspecting that building after an earthquake. When convolved with site hazard, the fragility curves for tagging conditions can be useful for a variety of applications, such as estimation of the likelihood of downtime for buildings either as stand-alone units or as parts of a network. Post-earthquake occupancy restrictions play also an important role in the assessment of business interruption losses.

ACKNOWLEDGEMENTS

The PEER Lifelines Program funded the work presented in this paper, which is excerpted from guidelines prepared for Pacific Gas & Electric. The content of the guidelines greatly benefited from discussions with many individuals: Kent Ferre, Norman Abrahamson, and Lloyd Cluff of PG&E, Maryann Phipps of Estructure, William Holmes and Joseph Maffei of Rutherford & Chekene, Robert Kennedy of SMC , Nicolas Luco of AIR Worldwide, and Graham Powell formerly at UC Berkeley.

REFERENCES

1. ATC-20. "*Procedures for Post earthquake Safety Evaluation of Buildings*", Applied Technology Council, 555 Twin Dolphin Drive, Suite 550, Redwood City, California 94065, 1989.
2. FEMA 350-352. "*Recommended Seismic Design Criteria for New Steel Moment-Frame Buildings (350); Recommended Seismic Evaluation and Upgrade Criteria for Existing Welded Steel Moment-Frame Buildings (351); Recommended Post-earthquake Evaluation and Repair Criteria for Welded Steel Moment-Frame Buildings (352)*", SAC Joint Venture, Sacramento, California, July, 2000.
3. Bazzurro P, Cornell CA, Menun C, and Motahari M. "Advanced Seismic Assessment Guidelines", Report Prepared for PG&E, PEER Lifelines Program, Task 501, Draft 1, February 28, 2002.
4. FEMA 356. "*Prestandard and Commentary for the seismic rehabilitation of buildings*", Building Seismic Safety Council, Washington, D.C., November, 2000.
5. Luco N, Bazzurro P, and Abrahamson N. "Scaling of Earthquake Ground Motions and Nonlinear Structural Responses", *Proceedings of 13th WCEE*, Paper No.2404, Vancouver, Canada, August, 2004.
6. Luco N, Bazzurro P, and Cornell CA. "Dynamic Versus Static Computation of the Capacity of a Mainshock Damaged SMRF Building to Withstand an Aftershock", *Proceedings of 13th WCEE*, Paper No.2405, Vancouver, Canada, August, 2004.
7. Vamvatsikos D, and Cornell CA. "Practical Estimation of the Seismic Demand and Capacity of Oscillators with Multi-Linear Static Pushovers through Incremental Dynamic Analysis", *Proceedings of 7th U.S. National Conference on Earthquake Engineering*, Boston, July 21-25, 2002.
8. Vamvatsikos D, and Cornell CA. "Incremental Dynamic Analysis", *Earthquake Engineering and Structural Dynamics*, Vol. 31, No. 3, John Wiley & Sons, Ltd., New York, April, 2001.
9. RAM Perform 2D. "User Manual", RAM International, Carlsbad, CA, October, 2000.
10. Maffei J, Mohr DS, and Holmes WT. "Test Application of Advanced Seismic Assessment Guidelines 3-Story Steel Moment-Resisting Frame Building", Report Prepared for PG&E/PEER Lifelines Program, Task 508, Draft 1, December 13, 2002.
11. HAZUS. "*Natural Hazard Estimation Methodology*", FEMA,1999.
URL: (http://www.fema.gov/hazus/)
12. Wiemer S. "Introducing probabilistic aftershock hazard mapping", *Geophysical Research Letters,* Vol. 27**,** pp. 3405-3408, 2000.
13. Yeo, G-L., and Cornell CA. "Building Tagging Criteria Based on Aftershock PSHA", *Proceedings of 13th WCEE*, Paper No.3283, Vancouver, Canada, August, 2004.